Cell Reports

Report

Tet2 Rescues Age-Related Regenerative Decline and Enhances Cognitive Function in the Adult Mouse Brain

Graphical Abstract

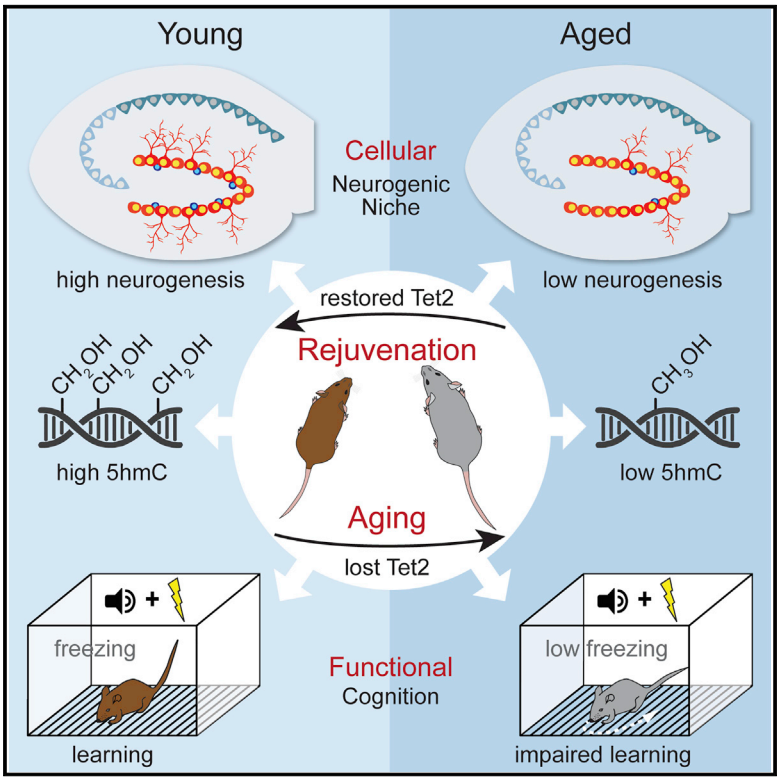

Authors

Geraldine Gontier, Manasi Iyer, Jeremy M. Shea, Gregor Bieri, Elizabeth G. Wheatley, Miguel Ramalho-Santos, Saul A. Villeda

Correspondence

saul.villeda@ucsf.edu

In Brief

Gontier et al. find a link between Tet2 and neurogenic rejuvenation. Age-related loss of hippocampal Tet2 and 5hmC associates with decreased neurogenesis. Mimicking age-related loss of Tet2 in the young mouse hippocampus decreases neurogenesis and impairs cognition. Restoring Tet2 in the mature hippocampus rejuvenates regenerative capacity and enhances cognition.

Highlights

- Loss of Tet2 and 5hmC in the aged hippocampus associates with regenerative decline
- Decreasing Tet2 in the young mouse hippocampus impairs neurogenesis and cognition
- Heterochronic parabiosis restores Tet2 in the aged hippocampus
- Restoring Tet2 in the mature hippocampus rescues neurogenesis and enhances cognition

Data and Software Availability

GSE102473

Gontier et al., 2018, Cell Reports *22*, 1974–1981
February 20, 2018
https://doi.org/10.1016/j.celrep.2018.02.001

CellPress

OPEN ACCESS
CellPress

Cell Reports
Report

Tet2 Rescues Age-Related Regenerative Decline and Enhances Cognitive Function in the Adult Mouse Brain

Geraldine Gontier,[1] Manasi Iyer,[1] Jeremy M. Shea,[1] Gregor Bieri,[1] Elizabeth G. Wheatley,[1,2] Miguel Ramalho-Santos,[3] and Saul A. Villeda[1,2,4,5,6,*]

[1]Department of Anatomy, University of California, San Francisco, San Francisco, CA 94143, USA
[2]Developmental and Stem Cell Biology Graduate Program, University of California, San Francisco, San Francisco, CA 94143, USA
[3]Department of Obstetrics, Gynecology and Reproductive Sciences, University of California, San Francisco, San Francisco, CA 94143, USA
[4]Department of Physical Therapy and Rehabilitation Science, University of California, San Francisco, San Francisco, CA 94143, USA
[5]The Eli and Edythe Broad Center for Regeneration Medicine and Stem Cell Research, University of California, San Francisco, San Francisco, CA 94143, USA
[6]Lead Contact
*Correspondence: saul.villeda@ucsf.edu
https://doi.org/10.1016/j.celrep.2018.02.001

SUMMARY

Restoring adult stem cell function provides an exciting approach for rejuvenating the aging brain. However, molecular mechanisms mediating neurogenic rejuvenation remain elusive. Here we report that the enzyme ten eleven translocation methylcytosine dioxygenase 2 (Tet2), which catalyzes the production of 5-hydroxymethylcytosine (5hmC), rescues age-related decline in adult neurogenesis and enhances cognition in mice. We detected a decrease in Tet2 expression and 5hmC levels in the aged hippocampus associated with adult neurogenesis. Mimicking an aged condition in young adults by abrogating Tet2 expression within the hippocampal neurogenic niche, or adult neural stem cells, decreased neurogenesis and impaired learning and memory. In a heterochronic parabiosis rejuvenation model, hippocampal Tet2 expression was restored. Overexpressing Tet2 in the hippocampal neurogenic niche of mature adults increased 5hmC associated with neurogenic processes, offset the precipitous age-related decline in neurogenesis, and enhanced learning and memory. Our data identify Tet2 as a key molecular mediator of neurogenic rejuvenation.

INTRODUCTION

During aging, the number of neural stem/progenitor cells (NPCs), and subsequently neurogenesis, precipitously declines in the subgranular zone of the dentate gyrus (DG) in the hippocampus (Fan et al., 2017). Mounting evidence in animal models indicates the potential for rejuvenation of regenerative and cognitive functions in the aging brain through interventions, such as heterochronic parabiosis (which exposes aged animals to young blood) (Fan et al., 2017; Katsimpardi et al., 2014; Villeda et al., 2011). However, the ability to utilize this neurogenic potential is predicated on identifying molecular targets that reverse the effects of aging in the brain.

Recent studies have begun to link changes in the functions of epigenetic mediators, such as those necessary for covalent DNA modifications, to age-related regenerative decline (Beerman and Rossi, 2015; Brunet and Rando, 2017). Interestingly ten eleven translocation methylcytosine dioxygenase 2 (Tet2), which catalyzes the oxidation of 5-methylcytosine (5mC) to 5-hydroxymethylcytosine (5hmC), is emerging as a potential epigenetic regulator of aging (Burgess, 2015). Human genetic studies identified an increased frequency of somatic *TET2* mutations with age that are associated with elevated risk for aging-associated disorders, such as cancer, cardiovascular disease, and stroke (Burgess, 2015; Jaiswal et al., 2014; Nadarajah et al., 2015). Notwithstanding, the involvement of Tet2 in mediating the aging process in the adult brain has yet to be investigated. While Tet proteins and 5hmC are highly expressed in the brain (Hahn et al., 2013; Kriaucionis and Heintz, 2009; Szulwach et al., 2011), with Tet1 and Tet3 implicated in proper brain function (Kaas et al., 2013; Li et al., 2014; Rudenko et al., 2013; Zhang et al., 2013), the role of Tet2 remains relatively unexplored.

Here we demonstrate that Tet2 offsets age-related neurogenic decline and enhances cognition in the hippocampus of adult mice. We detect an age-dependent decrease in the levels of Tet2 and 5hmC in the aging hippocampus coincident with decreased adult neurogenesis. Mimicking an age-related loss of Tet2 in the adult neurogenic niche of the hippocampus, or adult NPCs, impairs regenerative capacity and associated hippocampal-dependent learning and memory processes. Conversely, increasing Tet2 in the hippocampus of mature animals increases 5hmC associated with neurogenic processes, restores adult neurogenesis to youthful levels, and enhances cognitive function. These findings indicate that Tet2-mediated hydroxymethylation regulates age-related regenerative decline in the aging hippocampus, with functional implications for neurogenic rejuvenation.

RESULTS

Tet2 and 5hmC Levels Decrease in the Aged Hippocampus and Are Associated with Neurogenic Processes

We characterized changes in the levels of Tet2 mRNA in the hippocampus and cortex of normal young and aged animals by qPCR, and we detected an age-related decrease in Tet2 expression within the aged hippocampus (Figures 1A and 1B). We examined changes in hippocampal 5hmC and 5mC levels by slot blot and immunohistochemical analysis, and we observed an age-related decrease in 5hmC (Figures 1C and 1D), but not 5mC (Figures S1A and S1B). To gain mechanistic insight into which genomic loci were affected by these changes, we performed antibody-based 5hmC immunoprecipitation combined with deep sequencing (hMeDIP-seq) in the young and aged hippocampus (Figures 1E and 1F; Figures S1C–S1H). We characterized differentially 5-hydroxymethylated regions (DhMRs) (Feng et al., 2012), and we identified 345 DhMRs lost, while detecting none gained, with age (Figure 1E; Table S1). Lost DhMRs were enriched in intragenic regions, in the aged compared to young hippocampus (Figure 1E), and we observed DhMR-associated genes were involved in neurogenic processes by gene ontology analysis (Figure 1F).

To further investigate the relationship between age-related changes in Tet2 expression and adult neurogenesis, we compared the temporal kinetics of decreased adult neurogenesis and Tet2 expression with age (Figures 1G–1I; Figure S1I). Adult neurogenesis and Tet2 expression were quantified in contralateral hippocampi of the same animals by immunohistochemical analysis and qPCR, respectively. We observed a precipitous decline in adult neurogenesis by 6 months of age in mature adults (Figures 1H and 1I; Figure S1I) that was paralleled by a sharp decrease in Tet2 expression (Figure 1G; Figure S1I). Altogether, these data raise the possibility that decreased Tet2 and 5hmC levels in the aging hippocampus are associated with age-related impairments in adult neurogenesis.

Reducing Tet2 in the Young Adult Hippocampus Impairs Neurogenesis

We next asked whether mimicking an age-related decline in Tet2 within the young adult hippocampus would impair neurogenesis. We first abrogated Tet2 expression in the young adult hippocampus utilizing an *in vivo* viral-mediated RNAi approach (Figure 2A). Young adult animals were stereotaxically injected with high-titer lentivirus (LV) encoding Tet2 or scramble control small hairpin RNA (shRNA) sequences into the DG of contralateral hippocampi, and Tet2 abrogation was confirmed *in vivo* (Figures S2A–S2C). No changes in Tet1 or Tet3 were detected (Figure S2D). Subsequently, we analyzed NPC function and maturation in an independent cohort of young adult animals by immunohistochemical analysis. Abrogation of Tet2 in the DG resulted in a significant decrease in the number of Sox2/GFAP-positive NPCs, Doublecortin (Dcx)-positive newly born neurons, Bromodeoxyuridine (BrdU)-positive cells, and BrdU/NeuN-positive mature differentiated neurons compared with the control contralateral DG (Figure 2B).

To gain mechanistic insight at a cellular level, we generated $Tet2^{floxf/lox}$ mice carrying an inducible *NestinCre-ERT*^{2} gene, in which *Tet2* is excised specifically in adult NPCs ($Tet2^{-/-}$) upon tamoxifen administration (Figure 2C; Figure S2E). We examined changes in neurogenesis in young adult $Tet2^{-/-}$ and littermate control ($Tet2^{floxf/lox}$) mice by immunohistochemical analysis. The absence of Tet2 expression in adult NPCs resulted in a selective decrease in the number of Dcx-positive newly born neurons, BrdU-positive cells, and BrdU/NeuN-positive mature differentiated neurons in $Tet2^{-/-}$ mice compared to $Tet2^{flox/flox}$ controls, without altering the number of Nestin-positive NPCs (Figure 2D). This decrease in newly born and mature neurons is consistent with increased levels of 5hmC upon neuronal differentiation *in vivo* (Figure S2F). Collectively, our *in vivo* RNAi and genetic data suggest an involvement of Tet2 in regulating adult neurogenesis at both the levels of the neurogenic niche and adult NPCs.

Reducing Tet2 in the Young Adult Hippocampus Impairs Cognitive Function

To investigate whether decreased Tet2 in the young adult DG, or loss of Tet2 in adult NPCs, impaired cognitive processes, hippocampal-dependent learning and memory were assessed using radial arm water maze (RAWM) and contextual fear-conditioning paradigms (Figure 3A). To test the effect of decreased Tet2 in the adult DG, young adult animals were given bilateral stereotaxic injections into the hippocampi of high-titer LV encoding Tet2 shRNA or scramble control sequences (Figure 3B). To test the effect of selective loss of Tet2 in adult NPCs, we utilized young adult NPC $Tet2^{-/-}$ and littermate control $Tet2^{flox/flox}$ mice (Figure 3E). All mice showed similar learning capacity during the training phase of the RAWM (Figures 3D and 3G). Abrogation of Tet2 in the adult DG resulted in significantly more errors in locating the target platform during both short-term (Figure 3D; Figure S3B) and long-term (Figure 3D; Figure S3C) learning and memory testing compared to control conditions. Interestingly, selective loss of Tet2 in adult NPCs resulted in impairments only during long-term learning and memory testing compared to control mice (Figure 3G; Figures S3E and S3F). During fear conditioning training, mice exhibited no differences in baseline freezing time (Figures S3A and S3D). However, both abrogation of Tet2 in the adult DG and loss of Tet2 in adult NPCs resulted in decreased freezing time during contextual (Figures 3C and 3F), but not cued (Figures S3A and S3D), memory testing. These data demonstrate that decreased Tet2 in the adult neurogenic niche, or adult NPCs, impairs long-term hippocampal-dependent spatial learning and memory and associative fear memory acquisition.

Decreased Tet2 in the Aged Hippocampus Is Reversed in a Heterochronic Parabiosis Model of Brain Rejuvenation

Thus far, at a cellular level, our findings indicate that mimicking an age-related decline in Tet2 impairs adult neurogenesis. However, it remains an open question whether restoring Tet2 in the adult brain can rescue age-related regenerative decline. Using a model of heterochronic parabiosis, we and others have demonstrated that rejuvenation of adult neurogenesis is possible in the aged brain (Katsimpardi et al., 2014; Villeda et al., 2011). To gain insight into the potential involvement of Tet2 in neurogenic rejuvenation, we measured mRNA levels of

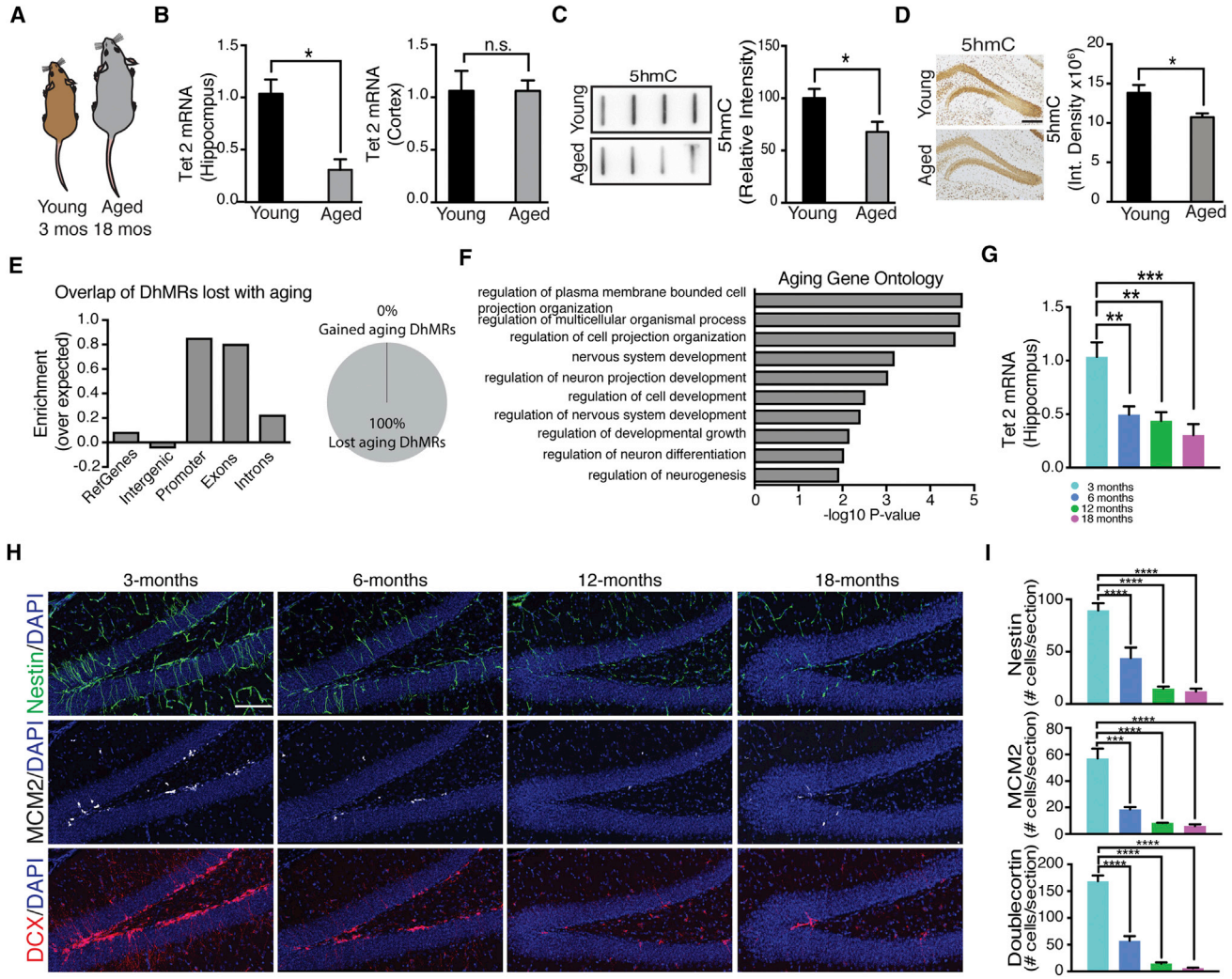

Figure 1. Tet2 Expression and 5hmC Levels Decline in the Aged Hippocampus and Are Associated with Neurogenic Processes

(A) Schematic of young adult (3-month-old) versus aged (18-month-old) mice.

(B) Quantitative reverse-transcription PCR of Tet2 mRNA from hippocampal and cortical lysates of young and aged mice (n = 5 per group; t test, *p < 0.05; n.s., not significant).

(C) Representative slot blot and quantification of isolated hippocampal DNA probed with anti-5hmC antibodies from young and aged mice (n = 4 per group; t test, *p < 0.05).

(D) Representative field and quantification of 5hmC expression in the dentate gyrus (DG) of the young and aged hippocampus (n = 4 per group; scale bar, 100 μm; t test, *p < 0.05).

(E) Association of regions of 5hmC lost during age with genomic elements (differentially 5-hydroxymethylated regions [DhMRs] lost between 3 and 18 months; 345 DhMRs at q = 0.05). Pie chart depicts overall loss and gain of DhMRs during aging.

(F) Top gene ontology terms for genes overlapping with age-associated 5hmC loss (>2-fold enrichment; ordered by p value).

(G) Reverse-transcription qPCR of Tet2 mRNA from hippocampal lysates of aging mice (n = 5; ANOVA with Dunnett's post hoc test, **p < 0.01).

(H and I) Neurogenesis was analyzed by immunostaining and confocal microscopy. Representative field (H) and quantification (I) of Nestin-positive, MCM2-positive, and Doublecortin (DCX)-positive cells in aging dentate gyrus (DG) at 3, 6, 12, and 18 months (n = 5; scale bar, 100 μm; ANOVA with Dunnett's post hoc test, ***p < 0.001 and ****p < 0.0001).

Data are represented as mean ± SEM. See also Figure S1.

Tet2 in the aged hippocampus after heterochronic parabiosis. We detected an increase of Tet2 in heterochronic parabionts after exposure to young blood compared to age-matched isochronic parabionts exposed to old blood (Figure 4A). No changes in Tet1 or Tet3 were observed (Figure S7A). These data implicate Tet2 in conditions of brain rejuvenation.

Restoring Tet2 in the Mature Adult Hippocampus Rescues Age-Related Regenerative Decline

To investigate whether restoring Tet2 in the adult hippocampal neurogenic niche could counteract age-related regenerative decline, we utilized an *in vivo* viral-mediated overexpression approach. Aging analysis demonstrated a concomitant

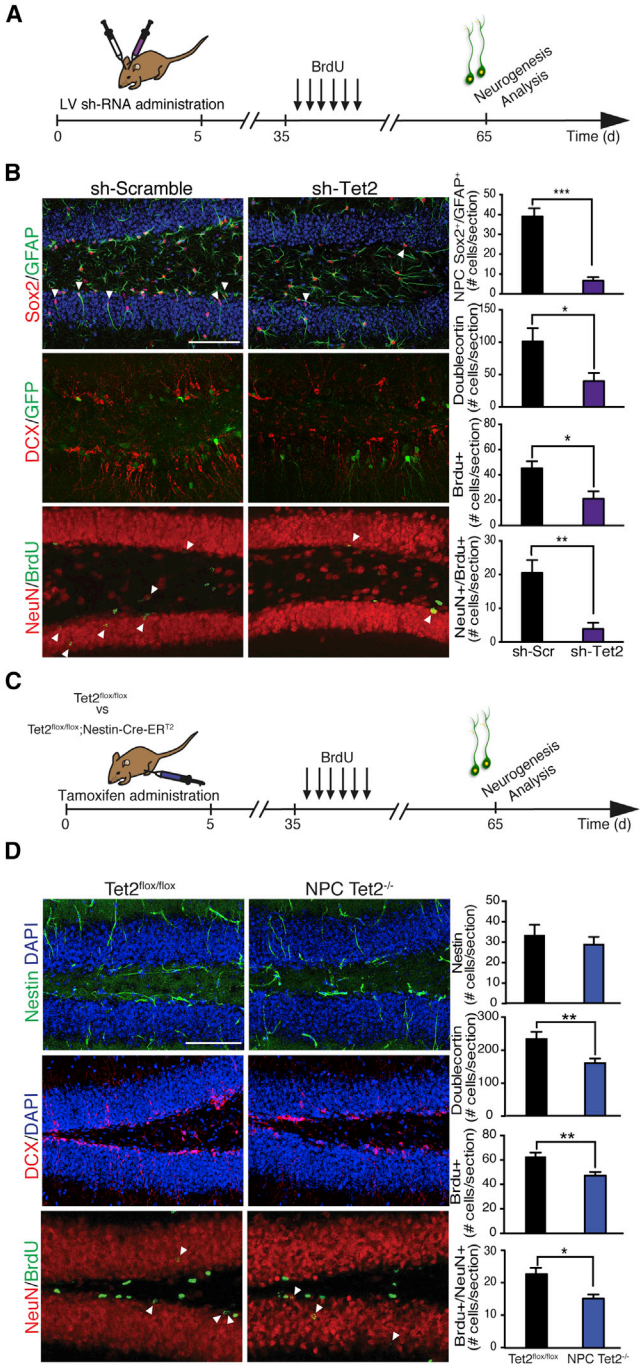

Figure 2. Abrogation of Tet2 in the Adult Dentate Gyrus or Loss of Tet2 in Adult NPCs Impairs Hippocampal Neurogenesis

(A and B) Young adult (3-month-old) mice were given unilateral stereotaxic injections of lentivirus (LV) encoding either shRNA targeting Tet2 or scramble control sequences in tandem with a GFP reporter into contralateral dentate gyrus (DG). Mice were administered BrdU by intraperitoneal injections for 6 days and euthanized 30 days later. Neurogenesis was analyzed by immunostaining and confocal microscopy.

(A) Schematic illustrating stereotaxic injection paradigm and experimental timeline.

(B) Representative field and quantification of GFAP/Sox2-positive, Doublecortin (Dcx)-positive, BrdU-positive, and NeuN/BrdU-positive cells (n = 5–9 per group; scale bar, 100 μm; t test, *p < 0.05, **p < 0.01, and***p < 0.001).

(C and D) A cell type-specific temporally controlled *Tet2*$^{flox/flox}$/*NestinCre-ERT*^{2} genetic model was generated, in which *Tet2* was excised selectively in adult neural stem/progenitor cells (NPCs) upon tamoxifen administration (*Tet2*$^{-/-}$). Neurogenesis was analyzed in young adult (3-month-old) NPC *Tet2*$^{-/-}$ and littermate control (*Tet2*$^{flox/flox}$) mice by immunostaining and confocal microscopy.

(C) Schematic illustrating tamoxifen injection paradigm and experimental timeline. Mice were administered BrdU by intraperitoneal injections for 6 days and euthanized 30 days later.

(D) Representative field and quantification of Nestin-positive, Dcx-positive, BrdU-positive, and NeuN/BrdU-positive cells (n = 7–8 per group; scale bar, 100 μm; t test, *p < 0.05, **p < 0.01, and ***p < 0.001).

Data are represented as mean ± SEM. See also Figure S2.

age-related decrease in adult neurogenesis and Tet2 expression in mature adult animals at 6 months of age (Figures 1G–1I). Correspondingly, mature adult animals at this age were stereotaxically injected with high-titer LV encoding Tet2 or control into the DG of contralateral hippocampi, and Tet2 overexpression was confirmed *in vivo* (Figure 4B; Figure S4B). No changes in Tet1 or Tet3 were detected (Figure S4C).

We performed hMeDIP-seq in the mature adult hippocampi following viral-mediated Tet2 overexpression (Figures 4C–4E; Figures S4D–S4H), and we found 558 DhMRs gained and 110 lost after Tet2 overexpression (Figure 4D; Table S2). We observed gained DhMRs enriched in intragenic regions (Figure 4D), and we identified associated neurogenic processes by gene ontology analysis (Figure 4E). We compared genes whose DhMRs were lost during aging with those gained by Tet2 overexpression, and we detected 39 overlapping genes (Table S3), of which 10 are involved in neurogenesis (Figure 4F).

Next, we examined whether restoring Tet2 was sufficient to rescue age-related decline in adult hippocampal neurogenesis by immunohistochemical analysis. We observed that increasing Tet2 in the mature adult DG resulted in a significant enhancement in the number of Sox2/GFAP-positive NPCs, Dcx-positive newly born neurons, BrdU-positive cells, and BrdU/NeuN-positive mature differentiated neurons in the DG compared with the control contralateral DG (Figure 4G). Excitingly, levels of adult neurogenesis achieved in the mature adult hippocampus by increased Tet2 mirrored levels normally observed in the young adult hippocampus (Figure 4G). We overexpressed Tet2 in the DG of young adult animals at 3 months of age, and we detected no changes in adult neurogenesis (Figure S4J). Our data indicate an age-dependent role for Tet2 in regulating regenerative decline in the aging brain.

Restoring Tet2 in the Mature Adult Hippocampus Enhances Cognitive Function

We next investigated the functional consequence of increasing Tet2 in the mature adult DG on cognition. Hippocampal-dependent learning and memory were assessed using RAWM and contextual fear-conditioning paradigms. Mature adult animals were given bilateral stereotaxic injections of high-titer LV encoding Tet2 or control into the DG of the hippocampus (Figure 4H; Figures S4K and S4L). All mice showed similar learning capacity during the training phase of the RAWM (Figure 4J), and no

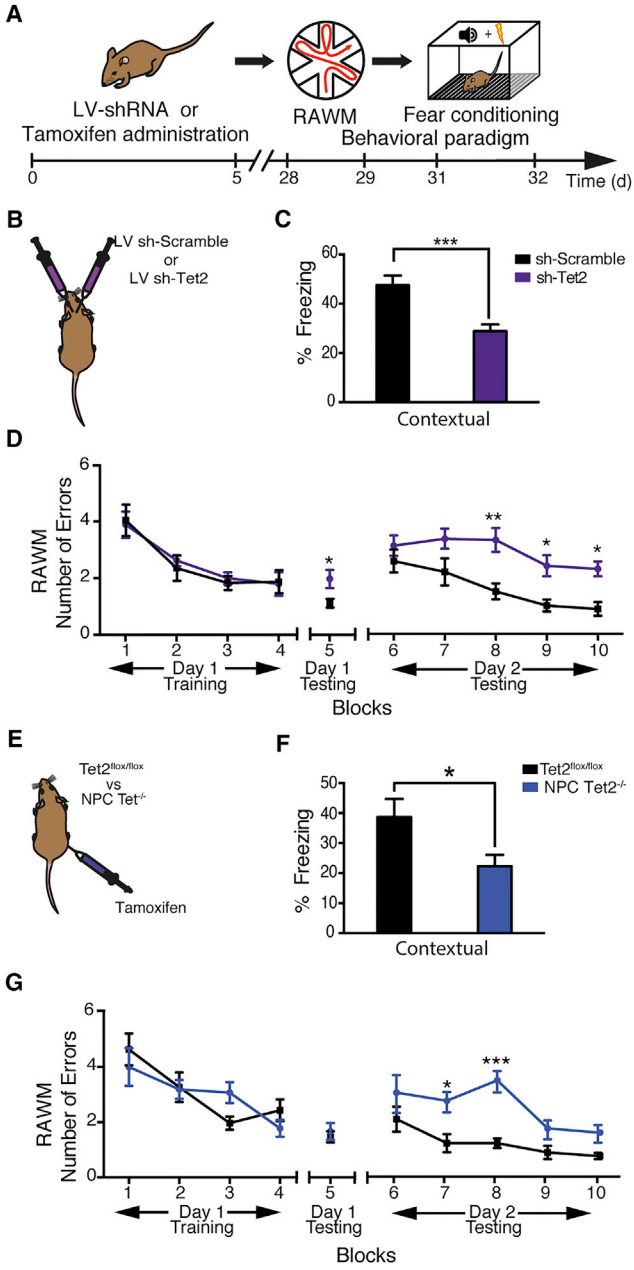

differences were detected in locating the target platform during short-term (Figure 4J; Figure S4N) and long-term (Figure 4J; Figure S4N) learning and memory testing. During fear conditioning training, mice exhibited no differences in baseline freezing time (Figure S4M). However, increased Tet2 expression in the mature adult DG resulted in increased freezing time during contextual (Figure 4I), but not cued (Figure S4M), memory testing. These data indicate that restoring Tet2 in the mature adult neurogenic niche is sufficient to enhance associative fear memory acquisition.

DISCUSSION

Cumulatively, our data indicate that age-related loss of Tet2 leads to decreased adult neurogenesis, with functional implications for cognitive impairment. Our *in vivo* RNAi and genetic data dissect the involvement of Tet2 in regulating adult neurogenesis at the level of the neurogenic niche and adult NPCs, pointing to complementary cell-autonomous and non-autonomous roles for Tet2 in regulating NPC function versus neuronal differentiation processes. Moreover, we demonstrate that increasing Tet2 in the hippocampus is sufficient to rescue the precipitous age-related regenerative decline observed in the mature adult brain and enhance associated cognitive processes. Ultimately, our data suggest that restoring Tet2 in the aging brain can promote rejuvenation.

Recently, it has been demonstrated that constitutive whole-body loss of Tet2 yields opposing effects on neurogenic processes, resulting in increased adult NPC proliferation but decreased neuronal differentiation (Li et al., 2017). In contrast, our data indicate that decreasing Tet2 expression acutely in the adult neurogenic niche impairs all stages of hippocampal neurogenesis, while loss of Tet2 in adult NPCs impairs neuronal differentiation processes. These data point to differential regulation of distinct stages of neurogenesis by Tet2 that arise from the loss of Tet2 at the level of the whole organism, neurogenic niche, and adult NSC during development versus adult ages. In the context of aging, our data implicate decreased Tet2 in the aging hippocampus with age-related regenerative decline.

While a causal link between age-related decreased neurogenesis and cognitive decline remains obfuscated (Drapeau et al., 2003; Merrill et al., 2003; Seib et al., 2013; Smith et al.,

Figure 3. Abrogation of Tet2 in the Adult Dentate Gyrus or Loss of Tet2 in Adult NPCs Impairs Hippocampal-Dependent Cognitive Function

(A) Schematic of experimental paradigm and cognitive testing timeline. Hippocampal-dependent learning and memory were assessed by radial arm water maze (RAWM) and contextual fear-conditioning paradigms.

(B) Young adult (3-month-old) wild-type mice were given bilateral stereotaxic injections of lentivirus (LV) encoding either shRNA targeting Tet2 (sh-Tet2) or scramble control sequences (sh-Scramble) into the dentate gyrus (DG).

(C) Associative fear memory was assessed in sh-Tet2- and sh-Scramble control-injected mice using contextual fear conditioning. Quantification of percentage freezing 24 hr after training is shown (n = 14 per group; t test, ***p < 0.001).

(D) Hippocampal-dependent spatial learning and memory were assessed in sh-Tet2- and sh-Scramble control-injected mice using RAWM. Quantification of the number of entry errors during RAWM training and testing is shown (n = 14 per group; repeated-measures ANOVA with Bonferroni post hoc correction, *p < 0.05 and **p < 0.01).

(E) Young adult $Tet2^{flox/flox}$/NestinCre-ERT^2 NPC-specific knockout ($Tet2^{-/-}$) or littermate control ($Tet2^{flox/flox}$) mice were administered tamoxifen. Data from 9–10 animals per group are shown.

(F) Associative fear memory was assessed in $Tet2^{-/-}$ and $Tet2^{flox/flox}$ control mice using contextual fear conditioning. Quantification of percentage freezing 24 hr after training is shown (n = 9–10 per group; t test, *p < 0.05).

(G) Hippocampal-dependent spatial learning and memory were assessed in in $Tet2^{-/-}$ and $Tet2^{flox/flox}$ control mice using RAWM. Quantification of the number of entry errors during RAWM training and testing is shown (n = 9–10 per group; repeated-measures ANOVA with Bonferroni post hoc correction, ***p < 0.001).

Data are represented as mean ± SEM. See also Figure S3.

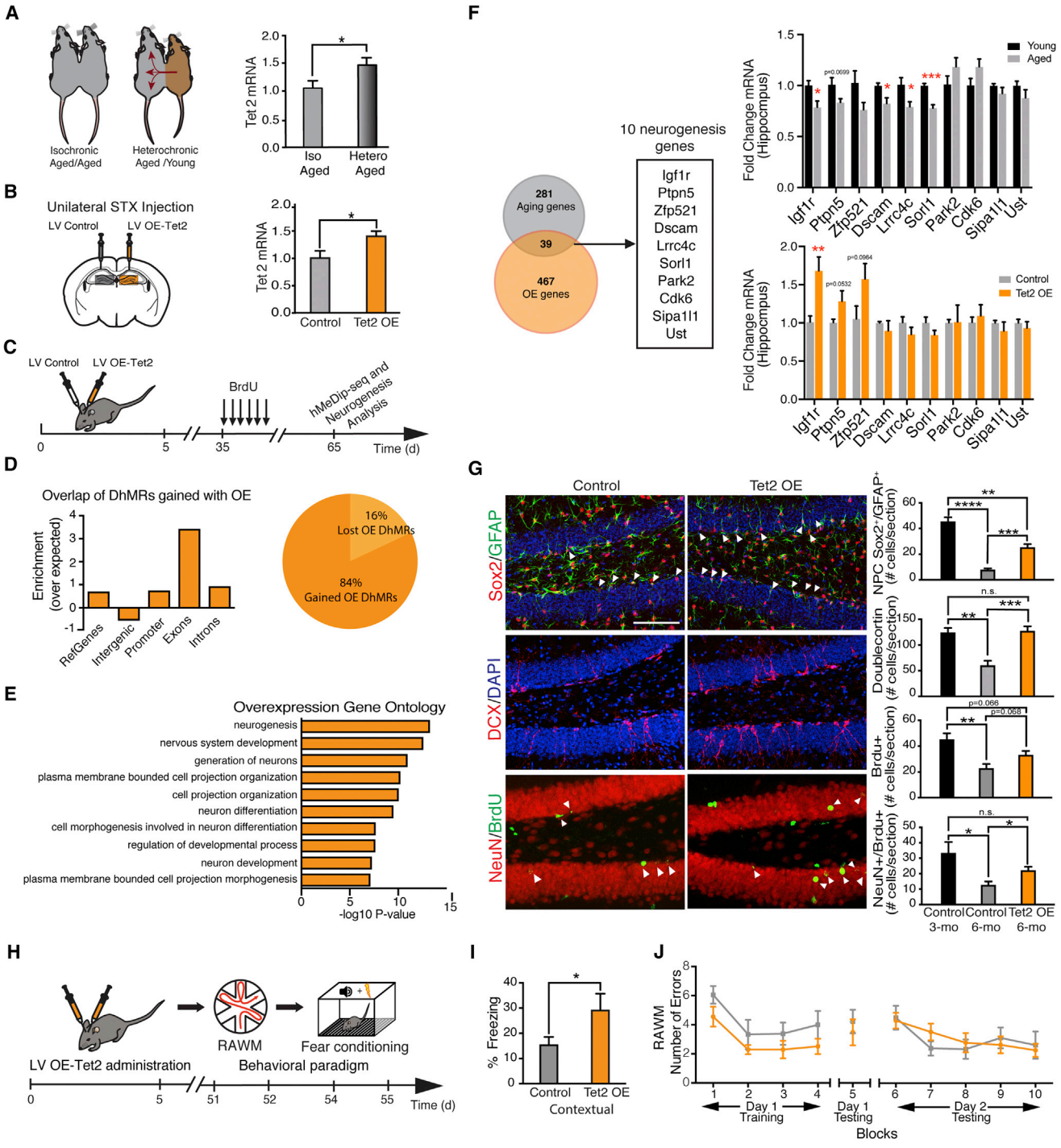

Figure 4. Increasing Tet2 in the Mature Adult Dentate Gyrus Rescues Age-Related Regenerative Decline and Enhances Cognitive Function

(A) Schematic and reverse-transcription qPCR of Tet2 mRNA from hippocampal lysates of aged (18-month-old) isochronic and heterochronic parabionts 5 weeks after parabiosis (n = 5 per group; t test, *p < 0.05).

(B) Mature adult (6-month-old) mice were given unilateral stereotaxic (STX) injections of lentivirus (LV) encoding Tet2 or control LV into contralateral dentate gyrus (DG). Schematic and qPCR of Tet2 mRNA from hippocampal lysates following STX injection are shown (n = 5 per group; t test, *p < 0.05).

(C) Schematic illustrating stereotaxic injection paradigm and experimental timeline.

(D) Association of regions of 5hmC gained after Tet2 overexpression with genomic elements (DhMRs gained; 558 DhMRs at q = 0.05). Pie chart depicts overall loss and gain of DhMRs after Tet2 overexpression (OE).

(E) Top gene ontology terms (2-fold enrichment, ordered by p value) for genes associated with gained DhMRs after Tet2 overexpression (OE).

(legend continued on next page)

2015), decreasing Tet2 within the young adult hippocampus, or loss of Tet2 in adult NPCs, resulted in cognitive impairments. Interestingly, impairments in short-term spatial learning and memory that are not typically associated with changes in adult neurogenesis were observed after Tet2 abrogation in the adult hippocampus, but not in adult NPCs, beginning to delineate complementary roles for Tet2 in regulating neurogenesis-dependent versus -independent cognitive functions. Collectively, our behavioral data identify a unique role for Tet2 in cognitive function distinct from other Tet family members, with previous studies implicating Tet1 and Tet3 in memory extinction but finding no role in long-term memory acquisition (Kaas et al., 2013; Li et al., 2014; Rudenko et al., 2013; Zhang et al., 2013).

Outside of the brain, aging-associated regenerative decline is also attributed to age-related dysfunction in tissue-specific adult stem cells throughout the body. Therefore, improving adult stem cell function provides an exciting approach for broadly rejuvenating regenerative capacity (Fan et al., 2017; Beerman and Rossi, 2015; Brunet and Rando, 2017). Mounting evidence indicates that interventions eliciting neurogenic rejuvenation (Katsimpardi et al., 2014; Villeda et al., 2011) concomitantly promote rejuvenation in peripheral tissues (Baht et al., 2015; Conboy et al., 2005; Sinha et al., 2014). Thus, our data raise the exciting possibility that rejuvenation of regenerative capacity could be promoted across tissues by targeting epigenetic regulators associated with the aging process. Moreover, the activities of several chromatin regulators are regulated by metabolites, notably Tet enzymes by vitamin C (Blaschke et al., 2013; Cimmino et al., 2017), raising the possibility that non-invasive metabolic interventions may further contribute to promoting epigenetic-mediated rejuvenation.

EXPERIMENTAL PROCEDURES

Further details and an outline of resources used in this work can be found in the Supplemental Experimental Procedures.

Animals

The following mouse lines were used: young (3-month-old), mature (6-month-old), and aged (18-month-old) male C57BL/6 mice (The Jackson Laboratory), *Tet2*$^{flox/flox}$ mice (The Jackson Laboratory), Gt(Rosa)26Sor$^{flox\text{-}stop\text{-}flox}$CAG-TdTomato mice (The Jackson Laboratory), and *NestinCreER*^{T2} mice (The Jackson Laboratory). Animal use was in accordance with institutional guidelines approved by the University of California, San Francisco Institutional Animal Care and Use Committee (IACUC).

Data and Statistical Analyses

All experiments were randomized and blinded by an independent researcher. Groups were un-blinded at the end of each experiment upon statistical analysis. The distribution of data in each set of experiments was tested for normality using D'Agostino-Pearson omnibus test or Shapiro-Wilk test. Statistical analysis was performed with Prism 7.0 software (GraphPad). Means between two groups were compared with two-tailed, unpaired Student's t test. Comparisons of means from multiple groups with each other or against one control group were analyzed with one-way ANOVA, followed by the appropriate post hoc tests (indicated in the figure legends).

DATA AND SOFTWARE AVAILABILITY

The accession number for the hMeDIP-seq data reported in this paper is GEO: GSE102473.

SUPPLEMENTAL INFORMATION

Supplemental Information includes Supplemental Experimental Procedures, four figures, and three tables and can be found with this article online at https://doi.org/10.1016/j.celrep.2018.02.001.

ACKNOWLEDGMENTS

We thank Dr. Barbara Panning for critical insight and technical assistance. Work was funded by the Irene Diamond Fund AFAR award, NIH Ruth L. Kirschstein NRSA fellowships (E.G.W., F31-AG050415 and J.M.S., F32-AG055292), a gift from Marc and Lynne Benioff (S.A.V.), the Glenn Foundation (S.A.V.), and the NIA (R01 AG053382 and R01 AG055797).

AUTHOR CONTRIBUTIONS

G.G. and S.A.V. developed the concept and designed experiments. G.G. collected and analyzed data. G.G. and M.I. performed histological and cognitive studies. J.M.S. performed 5meDIP-seq studies. G.B. and E.G.W. generated viral constructs. E.G.W. and S.A.V. performed parabiosis studies. M.R.-S. provided scientific expertise. G.B. generated schematics. G.G., J.M.S., and S.A.V. wrote the manuscript. S.A.V. supervised all aspects of the project. All authors had the opportunity to discuss results and comment on the manuscript.

DECLARATION OF INTERESTS

The authors declare no competing interests.

Received: September 27, 2017
Revised: November 20, 2017
Accepted: January 31, 2018
Published: February 20, 2018

(F) Venn diagram representing the overlap of genes paired with DhMRs from those lost during aging (3 months over 18 months) and those gained from Tet2 overexpression (OE over control). From the overlap, genes associated with neurogenesis using gene ontology are shown, and mRNA expression in hippocampal lysates was measured by qPCR (n = 5 per group; t test, *$p < 0.05$, **$p < 0.01$, and ***$p < 0.001$).

(G) Neurogenesis was analyzed by immunostaining and confocal microscopy in mature adult (6-month-old) animals after LV administration. As a reference, young adult (3-month-old) mice were given unilateral STX injections of control LV. All mice were administered BrdU by intraperitoneal injections for 6 days and euthanized 30 days later. Representative field and quantification of GFAP/Sox2-positive, Dcx-positive, BrdU-positive, and NeuN/BrdU-positive cells are shown (n = 5 per group; scale bar, 100 μm; t test, *$p < 0.05$, **$p < 0.01$, and ***$p < 0.001$).

(H) Schematic of experimental paradigm and cognitive testing timeline. Mature adult (6-month-old) wild-type mice were given bilateral stereotaxic (STX) injections of lentivirus (LV) encoding Tet2 or control LV into the dentate gyrus (DG).

(I) Associative fear memory was assessed using contextual fear conditioning. Quantification of percentage freezing 24 hr after training is shown (n = 12–15 per group; t test, ***$p < 0.001$).

(J) Hippocampal-dependent spatial learning and memory was assessed using RAWM. Quantification of the number of entry errors during RAWM training and testing is shown (n = 6–9 per group; repeated-measures ANOVA with Bonferroni post hoc correction).

Data are represented as mean ± SEM. See also Figure S4.

REFERENCES

Baht, G.S., Silkstone, D., Vi, L., Nadesan, P., Amani, Y., Whetstone, H., Wei, Q., and Alman, B.A. (2015). Erratum: Exposure to a youthful circulation rejuvenates bone repair through modulation of β-catenin. Nat. Commun. *6*, 7761.

Beerman, I., and Rossi, D.J. (2015). Epigenetic Control of Stem Cell Potential during Homeostasis, Aging, and Disease. Cell Stem Cell *16*, 613–625.

Blaschke, K., Ebata, K.T., Karimi, M.M., Zepeda-Martínez, J.A., Goyal, P., Mahapatra, S., Tam, A., Laird, D.J., Hirst, M., Rao, A., et al. (2013). Vitamin C induces Tet-dependent DNA demethylation and a blastocyst-like state in ES cells. Nature *500*, 222–226.

Brunet, A., and Rando, T.A. (2017). Interaction between epigenetic and metabolism in aging stem cells. Curr. Opin. Cell Biol. *45*, 1–7.

Burgess, D.J. (2015). Human genetics: somatic mutations linked to future disease risk. Nat. Rev. Genet. *16*, 69.

Cimmino, L., Dolgalev, I., Wang, Y., Yoshimi, A., Martin, G.H., Wang, J., Ng, V., Xia, B., Witkowski, M.T., Mitchell-Flack, M., et al. (2017). Restoration of TET2 function blocks aberrant self-renewal and leukemia progression. Cell *170*, 1079–1095.e20.

Conboy, I.M., Conboy, M.J., Wagers, A.J., Girma, E.R., Weissman, I.L., and Rando, T.A. (2005). Rejuvenation of aged progenitor cells by exposure to a young systemic environment. Nature *433*, 760–764.

Drapeau, E., Mayo, W., Aurousseau, C., Le Moal, M., Piazza, P.V., and Abrous, D.N. (2003). Spatial memory performances of aged rats in the water maze predict levels of hippocampal neurogenesis. Proc. Natl. Acad. Sci. USA *100*, 14385–14390.

Fan, X., Wheatley, E.G., and Villeda, S.A. (2017). Mechanisms of hippocampal aging and the potential for rejuvenation. Annu. Rev. Neurosci. *40*, 251–272.

Feng, J., Liu, T., Qin, B., Zhang, Y., and Liu, X.S. (2012). Identifying ChIP-seq enrichment using MACS. Nat. Protoc. *7*, 1728–1740.

Hahn, M.A., Qiu, R., Wu, X., Li, A.X., Zhang, H., Wang, J., Jui, J., Jin, S.G., Jiang, Y., Pfeifer, G.P., and Lu, Q. (2013). Dynamics of 5-hydroxymethylcytosine and chromatin marks in Mammalian neurogenesis. Cell Rep. *3*, 291–300.

Jaiswal, S., Fontanillas, P., Flannick, J., Manning, A., Grauman, P.V., Mar, B.G., Lindsley, R.C., Mermel, C.H., Burtt, N., Chavez, A., et al. (2014). Age-related clonal hematopoiesis associated with adverse outcomes. N. Engl. J. Med. *371*, 2488–2498.

Kaas, G.A., Zhong, C., Eason, D.E., Ross, D.L., Vachhani, R.V., Ming, G.L., King, J.R., Song, H., and Sweatt, J.D. (2013). TET1 controls CNS 5-methylcytosine hydroxylation, active DNA demethylation, gene transcription, and memory formation. Neuron *79*, 1086–1093.

Katsimpardi, L., Litterman, N.K., Schein, P.A., Miller, C.M., Loffredo, F.S., Wojtkiewicz, G.R., Chen, J.W., Lee, R.T., Wagers, A.J., and Rubin, L.L. (2014). Vascular and neurogenic rejuvenation of the aging mouse brain by young systemic factors. Science *344*, 630–634.

Kriaucionis, S., and Heintz, N. (2009). The nuclear DNA base 5-hydroxymethylcytosine is present in Purkinje neurons and the brain. Science *324*, 929–930.

Li, X., Wei, W., Zhao, Q.Y., Widagdo, J., Baker-Andresen, D., Flavell, C.R., D'Alessio, A., Zhang, Y., and Bredy, T.W. (2014). Neocortical Tet3-mediated accumulation of 5-hydroxymethylcytosine promotes rapid behavioral adaptation. Proc. Natl. Acad. Sci. USA *111*, 7120–7125.

Li, X., Yao, B., Chen, L., Kang, Y., Li, Y., Cheng, Y., Li, L., Lin, L., Wang, Z., Wang, M., et al. (2017). Ten-eleven translocation 2 interacts with forkhead box O3 and regulates adult neurogenesis. Nat. Commun. *8*, 15903.

Merrill, D.A., Karim, R., Darraq, M., Chiba, A.A., and Tuszynski, M.H. (2003). Hippocampal cell genesis does not correlate with spatial learning ability in aged rats. J. Comp. Neurol. *459*, 201–207.

Nadarajah, N., Meggendorfer, M., Kern, W., Haferlach, C., and Haferlach, T. (2015). Accumulation of somatic mutations as a function of aging: A study on 4843 TET2 mutated patients in comparison to their respective SNP pattern. Blood *126*, 4111.

Rudenko, A., Dawlaty, M.M., Seo, J., Cheng, A.W., Meng, J., Le, T., Faull, K.F., Jaenisch, R., and Tsai, L.H. (2013). Tet1 is critical for neuronal activity-regulated gene expression and memory extinction. Neuron *79*, 1109–1122.

Seib, D.R., Corsini, N.S., Ellwanger, K., Plaas, C., Mateos, A., Pitzer, C., Niehrs, C., Celikel, T., and Martin-Villalba, A. (2013). Loss of Dickkopf-1 restores neurogenesis in old age and counteracts cognitive decline. Cell Stem Cell *12*, 204–214.

Sinha, M., Jang, Y.C., Oh, J., Khong, D., Wu, E.Y., Manohar, R., Miller, C., Regalado, S.G., Loffredo, F.S., Pancoast, J.R., et al. (2014). Restoring systemic GDF11 levels reverses age-related dysfunction in mouse skeletal muscle. Science *344*, 649–652.

Smith, L.K., He, Y., Park, J.S., Bieri, G., Snethlage, C.E., Lin, K., Gontier, G., Wabl, R., Plambeck, K.E., Udeochu, J., et al. (2015). β2-microglobulin is a systemic pro-aging factor that impairs cognitive function and neurogenesis. Nat. Med. *21*, 932–937.

Szulwach, K.E., Li, X., Li, Y., Song, C.X., Wu, H., Dai, Q., Irier, H., Upadhyay, A.K., Gearing, M., Levey, A.I., et al. (2011). 5-hmC-mediated epigenetic dynamics during postnatal neurodevelopment and aging. Nat. Neurosci. *14*, 1607–1616.

Villeda, S.A., Luo, J., Mosher, K.I., Zou, B., Britschgi, M., Bieri, G., Stan, T.M., Fainberg, N., Ding, Z., Eggel, A., et al. (2011). The ageing systemic milieu negatively regulates neurogenesis and cognitive function. Nature *477*, 90–94.

Zhang, R.R., Cui, Q.Y., Murai, K., Lim, Y.C., Smith, Z.D., Jin, S., Ye, P., Rosa, L., Lee, Y.K., Wu, H.P., et al. (2013). Tet1 regulates adult hippocampal neurogenesis and cognition. Cell Stem Cell *13*, 237–245.

Cell Reports, Volume *22*

Supplemental Information

Tet2 Rescues Age-Related Regenerative Decline and Enhances Cognitive Function in the Adult Mouse Brain

Geraldine Gontier, Manasi Iyer, Jeremy M. Shea, Gregor Bieri, Elizabeth G. Wheatley, Miguel Ramalho-Santos, and Saul A. Villeda

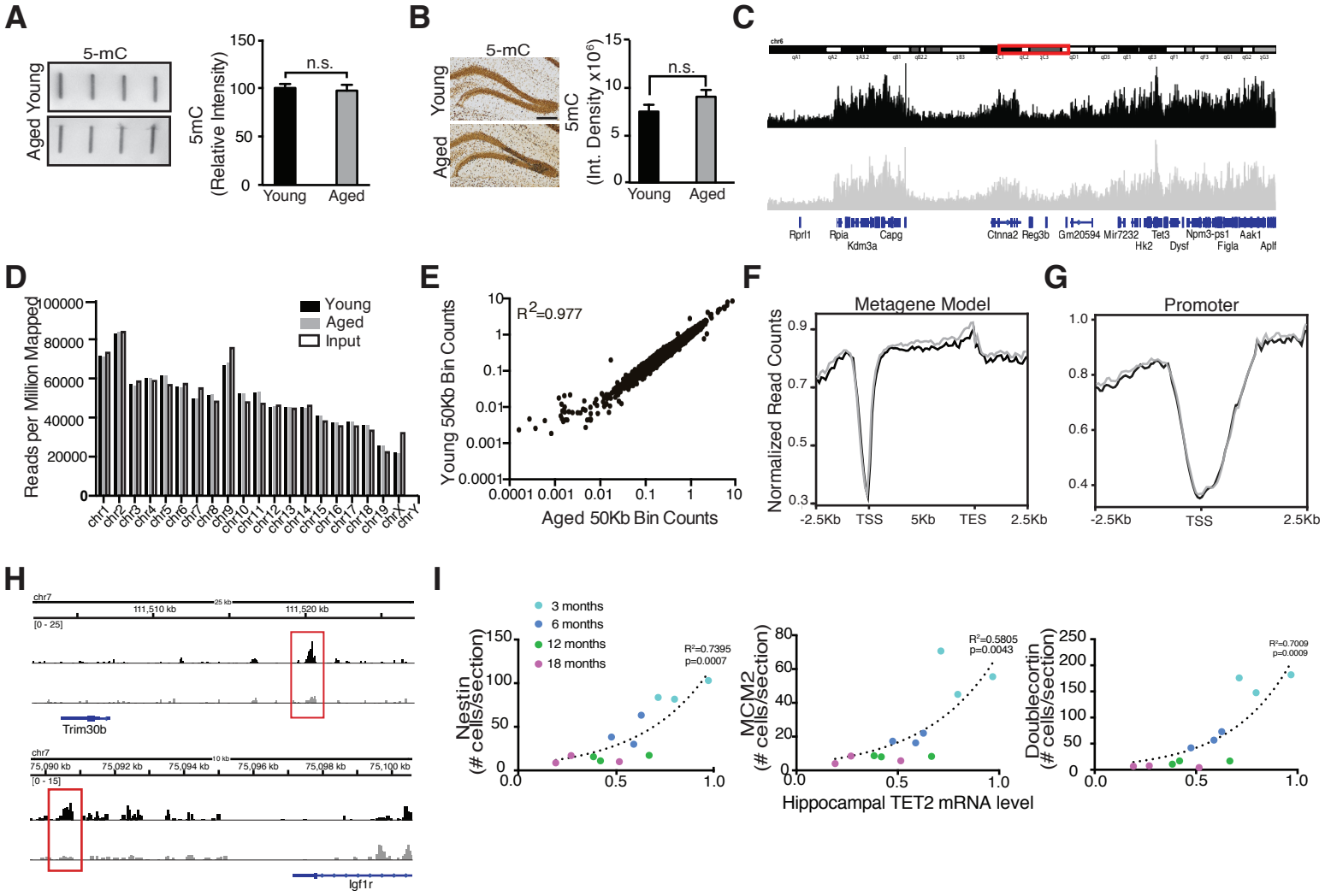

Figure S1. Characterization of 5mC levels, hMeDIP-sequencing, and adult neurogenesis in the young and aged hippocampus. Related to Figure 1.

A, Representative slot-blot and quantification of isolated hippocampal DNA probed with anti-5mc antibodies from young (3 months) and aged (18 months) mice. (n=4 per group; t-test; n.s. not significant)

B, Representative field and quantification of 5mc expression in the dentate gyrus (DG) of the young and aged hippocampus. (n=4 per group; scale bar, 100μm; t-test; n.s. not significant)

C, IGV Browser track of a 20mB region of chromosome 6. At the top is an ideogram of chromosome 6 with highlighted region in red box. Normalized read counts from young (3 months, black) and aged (18 months, grey) hippocampi from this region show increased reads over genes (signified at the bottom).

D, Chromosome coverage of hMeDIP-Seq reads from young, aged, and input samples normalized to reads per million mapped.

E, Scatterplot of young versus aged hippocampi using 50kb bins. Reads are normalized as FPKM.

F, Metagene read coverage in FPKM for RefSeq genes. The gene body was scaled to 5kb for all genes. 2.5kb upstream of the TSS and 2.5kb downstream of the TES are shown.

G, Read coverage in FPKM for RefSeq promoters. 2.5kb upstream and downstream of the TSS is shown.

H, Two examples of lost aging DhMRs that are proximal to Trim30b and Igf1r. Young (3 months, black) and aged (18 months, grey) samples are shown.

I, Temporal relationship between levels of adult neurogenesis and Tet2 expression in contralateral hippocampi with age (3, 6, 12, and 18 months). Quantification of Nestin-positive, MCM2-positive, and Doublecortin (DCX)-positive cells by immunohistochemistry was correlated with Tet2 mRNA levels assessed by quantitative reverse-transcription PCR. (n=3 per group)

Data are represented as mean±SEM.

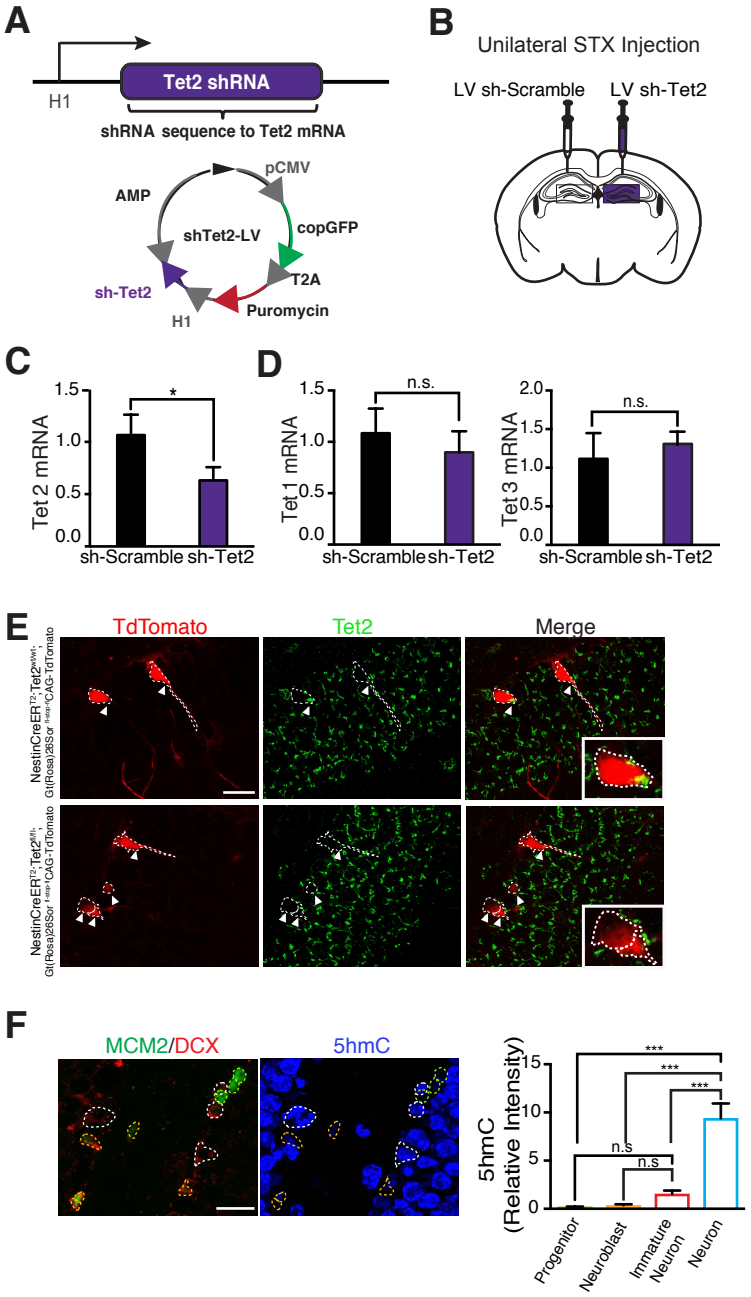

Figure S2. Abrogation of Tet2 by lentiviral-mediated shRNA approach and 5hmC expression during neuronal differentiation. Related to Figure 2.

A,B, Young adult (3 months) mice were given unilateral stereotaxic (STX) injections of lentivirus (LV) encoding either shRNA targeting Tet2 or scramble control sequences in tandem with a green florescent protein (GFP) reporter into contralateral dentate gyrus (DG). Schematic of lentiviral vector generated to express small hairpin RNAs (shRNA) targeting Tet2. Abbreviations: AMP, ampicillin, pCMV, cytomegalovirus promoter (A). Schematic illustrating unilateral STX injection paradigm into the DG (B).

C,D, Quantitative reverse-transcription PCR of Tet1, Tet2, and Tet3 mRNA from hippocampal lysates following STX injection. (n=5 per group; t-test; *P< 0.05, n.s. not significant)

E, A cell type specific temporally controlled Tet2wt/wt/NestinCre-ERT2/Gt(Rosa)26Sorflox-stop-floxCAG-TdTomato or Tet2flox/flox/Nestin-Cre-ERT2/Gt(Rosa)26Sorflox-stop-floxCAG-TdTomato genetic model was generated, in which TdTomato is expressed in adult neural stem/progenitor cells (NPCs) and Tet2flox/flox excised upon tamoxifen administration. Representative field of TdTomato-positive cells and Tet2 expression by immunostaining and confocal microscopy in the young adult (3 months) hippocampus (scale bar, 20μm).

F, Representative field and quantification of 5hmC expression in neural progenitors (MCM2+/DCX-), neuroblasts (MCM2+DCX+), immature neurons (MCM2-DCX+) and mature neurons by immunostaining and confocal microscopy in the young adult (3 months) hippocampus. (n=4; scale bar, 20μm; ANOVA with Dunnett's post hoc test; ***P<0.001, n.s. not significant)

Data are represented as mean±SEM.

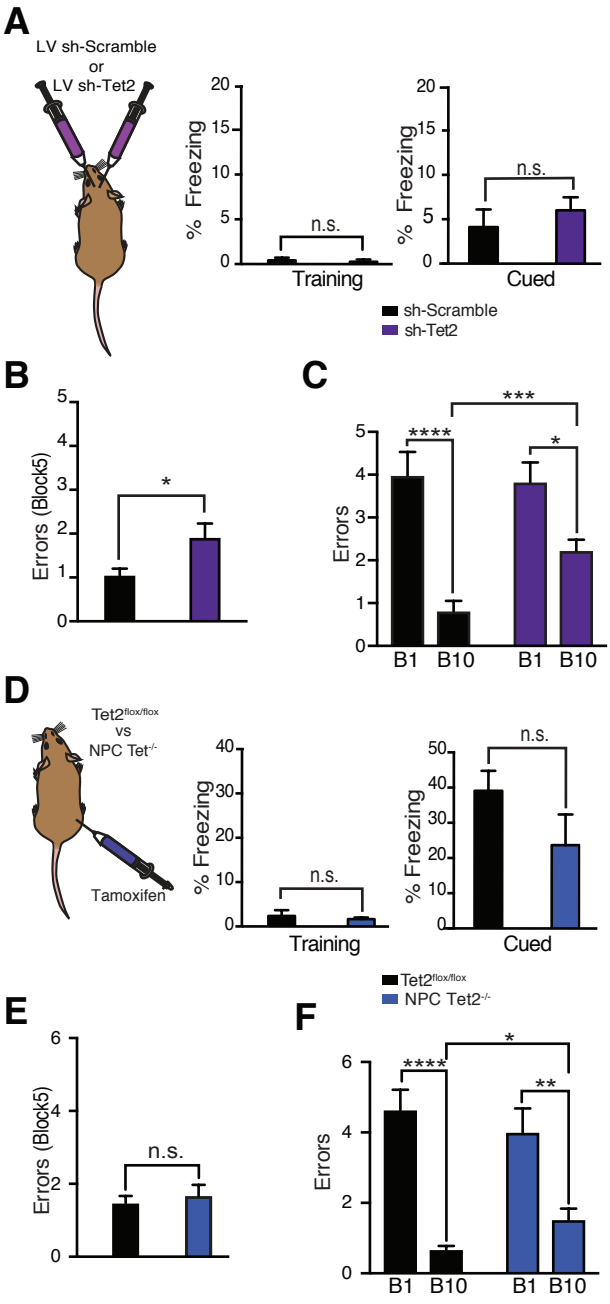

Figure S3: Abrogation of Tet2 in the adult dentate gyrus, but not loss of Tet2 in adult NPCs, selectively impairs short-term hippocampal-dependent spatial memory. Related to Figure 3.

A, Young adult (3 months) wild type mice were given bilateral stereotaxic injections of lentivirus (LV) encoding either shRNA targeting Tet2 (sh-Tet2) or scramble control sequences (sh-Scramble) into the dentate gyrus (DG). Cued fear memory was assessed in sh-Tet2 and sh-Scramble control injected mice using contextual fear conditioning. Quantification of percent freezing 24 hours after training. (n=14 per group; t-test; n.s not significant; t-test)

B,C, Hippocampal-dependent spatial learning and memory was assessed in sh-Tet2 and sh-Scramble control injected mice using RAWM. Quantification of the number of entry errors during RAWM short-term (B) and long-term (C) learning and memory testing. (n=14 per group; t-test; *P<0.05, ***P< 0.001, ****P< 0.0001)

D, Young adult Tet2flox/flox/NestinCre-ERT2 NPC-specific knockout (Tet2-/-) or littermate control (Tet2flox/flox) mice were administered tamoxifen. Cued fear memory was assessed in Tet2-/- and Tet2flox/flox control mice using contextual fear conditioning. Quantification of percent freezing 24 hours after training. (n=9-10 per group; t-test; n.s not significant)

E,F, Hippocampal-dependent spatial learning and memory was assessed in in Tet2-/- and Tet2flox/flox control mice using RAWM. Quantification of the number of entry errors during RAWM short-term (E) and long-term (F) learning and memory testing. (n=9-10 per group; t-test; *P<0.05, **P<0.01, ****P<0.0001, n.s not significant)

Data are represented as mean±SEM

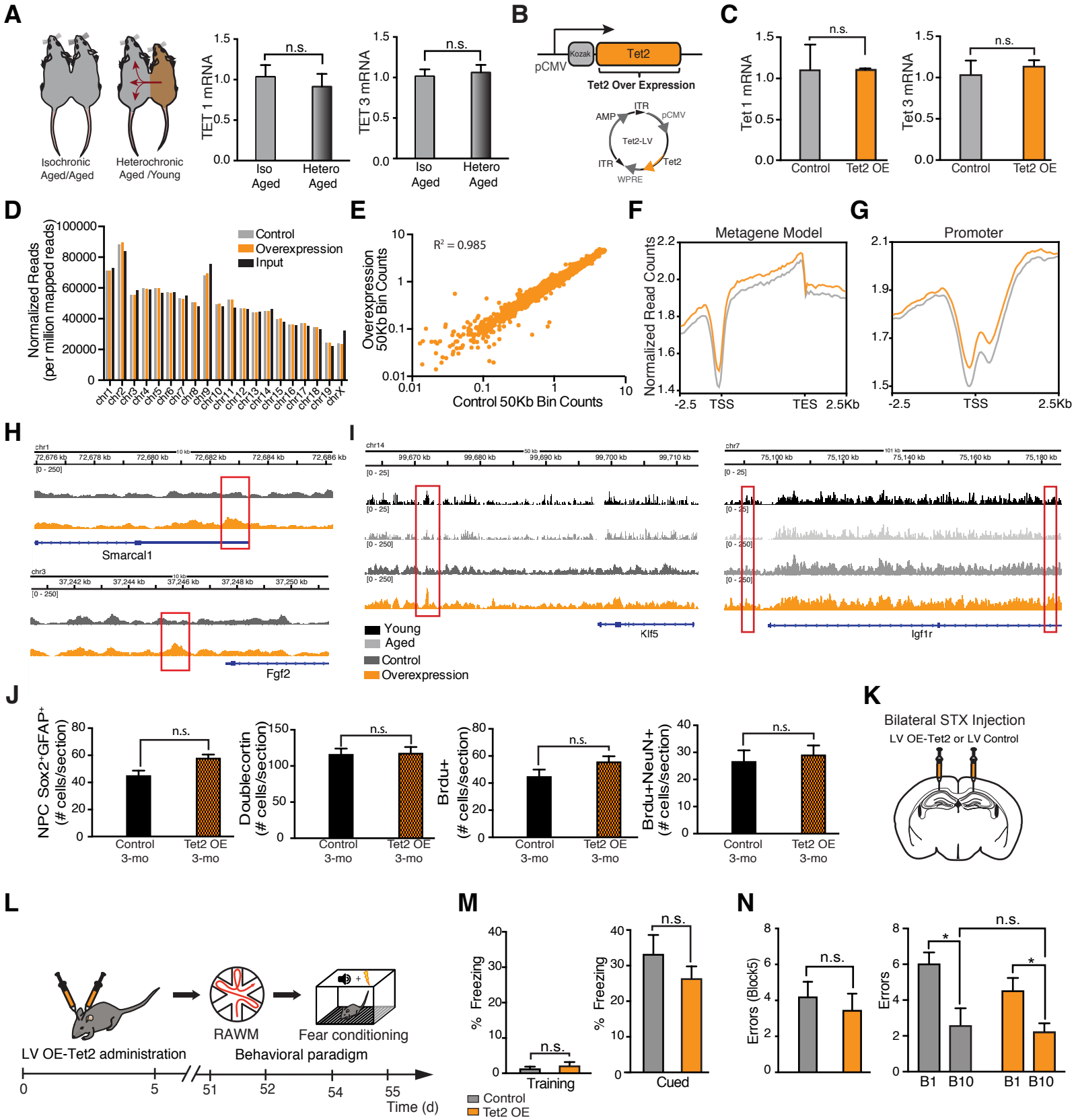

Figure S4. Characterization of hMeDIP-sequencing, adult neurogenesis, and cognitive function in the mature hippocampus following Tet2 overexpression. Related to Figure 4.

A, Schematic and quantitative reverse-transcription PCR of Tet2 mRNA from hippocampal lysates of aged (18 months) isochronic and heterochronic parabionts five weeks after parabiosis. (n= 5 per group; t-test; n.s not significant)

B,C, Mature adult (6 months) mice were given unilateral stereotaxic (STX) injections of lentivirus (LV) encoding Tet2 or control LV into contralateral dentate gyrus (DG). Schematic of lentiviral vector generated to overexpress Tet2. Abbreviations: AMP, ampicillin, pCMV, cytomegalovirus promoter (**B**). Quantitative reverse-transcription PCR of Tet1 and Tet3 mRNA from hippocampal lysates following STX injection (**C**). (n=5 per group; t-test; n.s. not significant)

D, Chromosome coverage of hMeDIP-Seq reads from control (dark grey), overexpression (orange), and input samples (black) normalized to reads per million mapped.
E, Scatterplot of control versus overexpression hippocampi using 50kb bins. Reads are normalized as FPKM.
F, Metagene read coverage in FPKM for RefSeq genes of control (dark grey) and Tet2 overexpression (orange). The gene body was scaled to 5kb for all genes. 2.5kb upstream of the TSS and 2.5kb downstream of the TES are shown.
G, Read coverage in FPKM for RefSeq promoters. 2.5kb upstream and downstream of the TSS is shown.
H, Two examples of DhMRs that were gained after Tet2 overexpression.
I, Two examples of genes that were associated with DhMRs that were lost with aging and gained after Tet2 overexpression are shown. In the example near Klf5, the DhMR is shared, while the example with Igf1r has two associated DhMRs. Examples of young (3 month, black), aged (18 month, grey), control (dark grey), and Tet2 overexpression (orange) samples are shown.
J, Young adult (3 months) mice were given unilateral stereotaxic (STX) injections of lentivirus (LV) encoding Tet2 or control LV into contralateral dentate gyrus (DG). Neurogenesis was analyzed by immunostaining and confocal microscopy after LV administration. All mice were administered BrdU by intraperitoneal injections for six days and euthanized 30 days later. Quantification of GFAP/Sox2-positive, Dcx-positive, BrdU-positive, and NeuN/BrdU-positive cells. (n=4 per group; t-test; n.s. not significant)
K,L, Schematic of experimental paradigm (**K**) and cognitive testing timeline (**L**). Mature adult (6 months) wild type mice were given bilateral stereotaxic (STX) injections of lentivirus (LV) encoding Tet2 or control LV into the dentate gyrus (DG). Hippocampal-dependent learning and memory was assessed by radial arm water maze (RAWM) and contextual fear conditioning paradigms.
M, Cued fear memory was assessed in Tet2 and control injected mice using contextual fear conditioning. Quantification of percent freezing 24 hours after training. (n=12-15 per group; t-test; ***P< 0.001)
N, Hippocampal-dependent spatial learning and memory was assessed in Tet2 and control injected mice using RAWM. Quantification of the number of entry errors during RAWM short-term and long-term learning and memory testing. (n=6-9 per group; t-test; *P<0.05, n.s not significant)
Data are represented as mean±SEM.

SUPPLEMENTAL EXPERIMENTAL PROCEDURES

Animal models. The following mouse lines were used: C57BL/6 (The Jackson Laboratory), C57BL/6 aged mice (The Jackson Laboratory), *Tet2*$^{flox/flox}$ (The Jackson Laboratory; stock number: 017573) mice, Gt(Rosa)26Sor$^{flox\text{-}stop\text{-}flox}$CAG-TdTomato (The Jackson Laboratory; stock number: 007905), and *NestinCreER*^{T2} mice (The Jackson Laboratory; stock number: 016261). All mice used were on a C57BL/6 genetic background. Mice carrying a *Tet2*$^{flox/lox}$ gene were crossed with mice carrying an inducible *NestinCre-ERT*^{2} gene to obtain *Tet2*$^{flox/flox}$/*NestinCreER*$^{T2+/0}$ mice. A subset of *Tet2*$^{flox/flox}$/*NestinCreER*$^{T2+/0}$ mice were crossed with Gt(Rosa)26Sor$^{flox\text{-}stop\text{-}flox}$CAG-TdTomato mice to obtain *Tet2*$^{flox/flox}$/*NestinCreER*$^{T2+/0}$/Gt(Rosa)26Sor$^{flox\text{-}stop\text{-}flox}$CAG-TdTomato. All studies were done in male mice. The numbers of mice used to result in statistically significant differences was calculated using standard power calculations with $\alpha = 0.05$ and a power of 0.8. We used an online tool (http://www.stat.uiowa.edu/~rlenth/Power/index.html) to calculate power and sample size on the basis of experience with the respective tests, variability of the assays and inter-individual differences within groups. Mice were housed under specific pathogen-free conditions under a 12-h light-dark cycle and all animal handling and use was in accordance with institutional guidelines approved by the University of California San Francisco Institutional Animal Care and Use Committee (IACUC) and the VA Palo Alto Committee on Animal Research.

PCR genotyping. Tet2 floxed and NestinCreER^{T2} alleles were genotyped from skin biopsies using PCR with Tet2 primers and NestinCreER^{T2} primers. Primers specific for the myogenin gene were included in the reaction as a control.

Primer Set	Forward Primer	Reverse Primer
Tet2 Floxed	AAGAATTGCTACAGGCCTGC	TTCTTTAGCCCTTGCTGAGC
Cre	GAACCTGATGGACATGTTCAGG	AGTGCGTTCGAACGCTAGAGCCTGT
Myogenin	TTACGTCCATCGTGGACAGC	TGGGCTGGGTGTTAGCCTTA

Tamoxifen administration. All experimental genetic mouse models (*Tet2*$^{flox/flox}$ control and *Tet2*$^{flox/flox}$/*NestinCreER*$^{T2+/0}$ mutant mice) received tamoxifen. At 2 months mice were administered tamoxifen to induce *Tet2* excision specifically in adult neural stem/progenitor cells termed NPC *Tet2*$^{-/-}$. Tamoxifen (T5648, Sigma-Aldrich) was dissolved in sunflower seed oil/ethanol (10:1) at 30 mg ml^{-1}, and was administered intraperitoneally at 180 mg kg^{-1} body weight once per day for 5 days. Animals were euthanized 2 months after the last injection.

RNA extraction, cDNA synthesis and qPCR. Total RNA was isolated using column from the RNeasy kit (QIAGEN, cat#74104). To quantify Tet2 mRNA expression levels, equal amounts of cDNA were synthesized using the High-Capacity cDNA Reverse Transcription kit (ThermoFisher Scientific, Cat# 4374966) and mixed with the Fast Taqman master mix (ThermoFisher Scientific), or the SYBR Fast mix (Kapa Biosystems), and Tet2 primers. GAPDH mRNA was amplified as an internal control. Quantitative RT-PCR was carried out in a CFX384 Real Time System (Bio-Rad).

Primer Set	reference	Forward Primer	Reverse Primer
Gapdh		AACAGCAACTCCCACTCTTC	CCTGTTGCTGTAGCCGTATT
Tet2		AGTAGGACTGAGAAGGGAAAGT	CGGTTGTGCTGTCATTTGTTT
Igf1r		GCCAGAAGTGGAGCAGAATAA	ACTTGTTGGCATTGAGGTAGG
Ptpn5		CGAGGAGATGAACGAGAAGTG	TCCGTGTGGATGACTTTCTG
Zfp521		AGTCCGATGAGAAGAAGACCTA	CTCATGGTTCAGCCCTTCAT
Dscam		GACACAGACCGAGCAAGAAG	TCCATCTTGGCGTGTTCATAG
Lrrc4c		GTCAAGACCGTGCATTCTTTC	TCTGGAGTTCAAACAGTTGTATTTC
Sorl1		CCTGACCAGGACTTGTTCTAC	AGCTTGCTTAGGCTGTACTC
Park2		CGATGCTCAACTTGGCTACT	TGGTACCTAGTGTACTGCTCTT
Cdk6		CTTCTGAAATGCCTGACGTTTAAT	GAGTTCAGGTTGTCCTTGTATCT
Sipa1l1		TCTGGACCTAGGACTTTCTACC	CACTCTGATGTCGCTTTCGT
Tet1	Mm01169087_m1		
Tet2	Mm00524395_m1		
Tet3	Mm00805756_m1		
Gapdh	Mm99999915_g1		

Slot blot analysis. Genomic DNA samples were prepared in TE buffer and then denatured in 0.0.5 M NaOH/12,5 mM EDTA at 95 °C for 10 min and followed by adding an equal volume of cold 2 M ammonium acetate (pH 7.2).

Denatured DNA samples were spotted on a charged nitrocellulose membrane in an assembled in the slot blot apparatus according to the manufacturer's instructions. The membrane was washed with TE buffer and ultraviolet-crosslinked for 3 min. Then the membrane was blocked with 1X PBS-0.1% Tween-20 (TBST) + 5% milk for 30 minutes at room temperature and incubated with rabbit anti-5hmC (1:500, Active Motif, Cat#39769) or mouse anti-5mC (1:500, Epigentek, Cat# A-1014-100) for HRP-conjugated secondary antibodies and enhanced chemiluminescence detection. Bands were analyzed using ChemiDoc (Bio-Rad) and quantified with ImageJ software analysis.

Viral plasmids. We generated lentiviruses that express shRNA sequences targeting Tet2 mRNA or full length Tet2. We used a lentiviral shRNA expression system (pGreenPuro shRNA, System Biosciences) according to the manufacturer's instructions. Tet2 shRNA sequences (Tet2, 5′- GTCTGAATCCATCTGTACATA-3′) were subcloned into the pGreenPuro vector. Scramble shRNA sequences (scramble, 5'- GGACGAACCTGCTGAGATAT-3') were subcloned as a control using the same protocol. Plasmid quality was tested with real time PCR analysis and sequencing. We generated lentiviral plasmids expressing full length Tet2 under a cytomegalovirus (CMV) promoter. Tet2 sequence was isolated using the Phusion Hot Start Flex DNA Polymerase (NEB,) using the following PCR primers: 5′- GAGGAGCAGAAGGAAGCAAGA-3′ and 5′- TGCCCTTGCATAGGATGCTC-3′, and subsequently subcloned into the pTB CMV plasmid using the restriction enzymes NheI and AscI.

Lentiviruses production. 293T cells were lipotransfected with 4:3:1 ug of lentiviral vector:psPax2:pCMV-VSVG. After 48 hours lentivirus-containing media was centrifuged and filtered to remove cellular debris. Media underwent utracentrifugation to concentrate virus. Lentiviral titers were between 2.5×10^7 and 5×10^8 viral particles per ml.

Stereotaxic injections. Animals were placed in a stereotaxic frame and anesthetized with 2% isoflurane (2 liters/min oxygen flow rate) delivered through an anesthesia nose cone. Ophthalmic eye ointment (Puralube Vet Ointment, Dechra) was applied to the cornea to prevent desiccation during surgery. The area around the incision was trimmed. Solutions were injected bilaterally into the DG of the dorsal hippocampi using the following coordinates: (from bregma) anterior = −2 mm, lateral = 1.5 mm, (from skull surface) height = −2.1 mm. A 2-µl volume was injected stereotaxically over 10 min (injection speed: 0.20 µl/min) using a 5-µl 26s-gauge Hamilton syringe. To limit reflux along the injection track, the needle was maintained *in situ* for 10 min, slowly pulled out halfway and kept in position for an additional 5 min. The skin was closed using silk suture. Each mouse was injected subcutaneously with analgesics. Mice were singly housed and monitored during recovery.

Parabiosis. Parabiosis surgery followed previously described procedures (Smith et al., 2015). Mirror-image incisions at the left and right flanks were made through the skin, and shorter incisions were made through the abdominal wall. The peritoneal openings of the adjacent parabionts were sutured together. Elbow and knee joints from each parabiont were sutured together and the skin of each mouse was stapled (9-mm Autoclip, Clay Adams) to the skin of the adjacent parabiont. Each mouse was injected subcutaneously with Baytril antibiotic and Buprenex as directed for pain and monitored during recovery. For overall health and maintenance behavior, several recovery characteristics were analyzed at various times after surgery, including paired weights and grooming behavior.

BrdU administration. For long-term BrdU labeling 50 mg/kg of BrdU (Sigma-Aldrich, Cat# B5002) was injected into mice once a day for 6 days and animals were euthanized 30 days after first administration.

Immunohistochemical Analysis. Tissue processing and immunohistochemistry was performed on free-floating sections according to standard published techniques (Smith et al., 2015). Briefly, mice were anesthetized with 87.5 mg/kg ketamine and 12.5 mg/mg xylazine and transcardially perfused with phosphate buffer saline. Brains were removed and fixed in phosphate-buffered 4% paraformaldehyde, pH 7.4, at 4 °C for 48 h before they were sunk through 30% sucrose for cryoprotection. Brains were then sectioned coronally at 40 µm with a cryomicrotome (Leica Camera, Inc.) and stored in cryoprotective medium. Primary antibodies were: goat anti-DCX (1:7500; Santa Cruz Biotechnology; sc-8066), rat anti-BrdU (1:1000, Abcam, AB6326), mouse anti-Nestin (1:200; Millipore; MAB353), mouse anti-MCM2 (1:250, BD Biosciences; 610700), mouse anti-NeuN (1:1000, Millipore, MAB377), rabbit anti-GFAP (1:1000; DAKO; Z0334), goat anti-Sox2 (1:200, Santa Cruz Biotechnology, sc17320), rabbit anti-GFP (1:10,000, Thermoscientific, PA5-22688), rabbit anti-5hmC (1:500, Active Motif, 39769), mouse anti-5mC (1:500, Epigentek, A-1014-100), and rabbit anti-Tet2 (1:500, Proteintech, 21207-1-AP). After overnight incubation, primary antibody staining was revealed using biotinylated secondary antibodies (Vector) and the ABC kit (Vector) with DAB (Sigma-Aldrich) or fluorescence-conjugated secondary antibodies (Life Technologies). For BrdU labeling, brain sections were pre-treated with 2 N HCl at 37 °C for 30 min and washed three times with Tris-buffered saline with

Tween (TBST) before incubation with primary antibody. For Nestin, MCM2, 5mC, 5hmC labeling, brain sections were pre-treated three times with 0.1M Citrate at 95 °C for 5 min, tree times and washed three times with TBST before incubation with primary antibody. To determine the number of mature differentiated neurons generated in the DG following first BrdU injection, we co-stained BrdU and the neuronal marker NeuN. All cells were counted in the DG of every sixth coronal hemibrain section through the hippocampus and analyzed by confocal microscopy using a Zeiss LSM800 microscope.

Contextual fear conditioning. In this task, mice learned to associate the environmental context (fear conditioning chamber) with an aversive stimulus (mild foot shock; unconditioned stimulus, US) enabling testing for hippocampal-dependent contextual fear conditioning. To also assess amygdala-dependent cued fear conditioning, the mild foot shock was paired with a light and tone cue (conditioned stimulus, CS). Conditioned fear was displayed as freezing behavior. Specific training parameters are as follows: tone duration is 30 seconds; level is 70 dB, 2 kHz; shock duration is 2 seconds; intensity is 0.6 mA. This intensity is not painful and can easily be tolerated but will generate an unpleasant feeling. More specifically, on day 1 each mouse was placed in a fear-conditioning chamber and allowed to explore for 2 min before delivery of a 30-second tone (70 dB) ending with a 2-second foot shock (0.6 mA). Two minutes later, a second CS-US pair was delivered. On day 2, each mouse was first placed in the fear-conditioning chamber containing the same exact context, but with no CS or foot shock. Freezing was analyzed for 1–2 minutes. One hour later, the mice were placed in a new context containing a different odor, cleaning solution, floor texture, chamber walls and shape. Animals were allowed to explore for 2 minutes before being re-exposed to the CS. Freezing was analyzed for 1–3 minutes using a FreezeScan video tracking system and software (Cleversys, Inc).

Radial arm water maze. Spatial learning and memory was assessed using the radial arm water maze (RAWM) paradigm according to the protocol described by (Alamed et al., 2006). In this task the goal arm location containing a platform remains constant throughout the training and testing phase, while the start arm is changed during each trial. Entry into an incorrect arm is scored as an error, and errors are averaged over training blocks (three consecutive trials). On day 1 during the training phase, mice are trained for 15 trails, with trials alternating between a visible and hidden platform for blocks 1-4 and then switching to only a hidden platform in block 5. On day 2 during the testing phase, mice are tested for 15 trials with a hidden platform for block 6-10. Investigators were blinded to genotype and treatment when scoring.

hMeDIP-Seq Library Preparation. For each library, 1.5ug of DNA was sonicated to 300-500 base pairs. DNA was precipitated, and resuspended in TE buffer. After end cleanup (Lucigen, ER81050) and A-tailing (Klenow Exo- NEB, M0212L), barcoded adapters were ligated onto the samples, followed by phenol/chloroform extraction and ethanol precipitation. Samples were then divided into input and immunoprecipitation samples. DNA was denatured by heating at 95°C for 10 minutes, followed by plunging the samples on ice. Ice-cold 10x hMeDIP buffer (100mM $NaPO_4$ pH 7.0, 1.4 mM NaCl, and 0.5% Triton X-100) was added to the immunoprecipitation sample to a final concentration of 1x. 2uL of 5hmC DNA antibody (Active Motif, 39769) was added to the samples. The samples were rotated overnight at 4°C. Protein A magnetic beads (NEB) were added to the reaction, and rotated at 4°C for 2 hours. The samples were collected on a magnetic rack, and the samples were washed three times (with 10 minute incubations) with 1x hMeDIP buffer. DNA was eluted from the beads by shaking the samples in lysis buffer (50mM Tris pH 8.0, 10mM EDTA, and 0.5% SDS) with proteinase K (100ug/ml) at 55°C for 3+ hours. The DNA was purified by phenol/chloroform extraction followed by ethanol precipitation. After purification, the libraries were PCR amplified (KAPA HiFi, kk2602) for 14-16 cycles using paired-end primers. Libraries were pooled and purified with 1.8X Agencourt AMpure XP beads (Beckman Coulter, A63881). Pooled libraries were quantified with KAPA Library Quantification Kit (kk4824).

Primer Set	Forward Primer	Reverse Primer
BC1-ACT	P-AGTAGATCGGAAGAGCGGTTCAGCAGGAATGCCGAG	ACACTCTTTCCCTACACGACGCTCTTCCGATCTACTT
BC2-TGA	P-TCAAGATCGGAAGAGCGGTTCAGCAGGAATGCCGAG	ACACTCTTTCCCTACACGACGCTCTTCCGATCTTGAT
BC3-CTG	P-CAGAGATCGGAAGAGCGGTTCAGCAGGAATGCCGAG	ACACTCTTTCCCTACACGACGCTCTTCCGATCTCTGT
BC4-GAC	P-GTCAGATCGGAAGAGCGGTTCAGCAGGAATGCCGAG	ACACTCTTTCCCTACACGACGCTCTTCCGATCTGACT
BC5-AGC	P-GCTAGATCGGAAGAGCGGTTCAGCAGGAATGCCGAG	ACACTCTTTCCCTACACGACGCTCTTCCGATCTAGCT
BC6-TCG	P-CGAAGATCGGAAGAGCGGTTCAGCAGGAATGCCGAG	ACACTCTTTCCCTACACGACGCTCTTCCGATCTTCGT
BC7-CAT	P-ATGAGATCGGAAGAGCGGTTCAGCAGGAATGCCGAG	ACACTCTTTCCCTACACGACGCTCTTCCGATCTCATT
BC8-GTA	P-TACAGATCGGAAGAGCGGTTCAGCAGGAATGCCGAG	ACACTCTTTCCCTACACGACGCTCTTCCGATCTGTAT
BC9-GAA	P-TTCAGATCGGAAGAGCGGTTCAGCAGGAATGCCGAG	ACACTCTTTCCCTACACGACGCTCTTCCGATCTGAAT
BC10-GTC	P-GACAGATCGGAAGAGCGGTTCAGCAGGAATGCCGAG	ACACTCTTTCCCTACACGACGCTCTTCCGATCTGTCT
BC11-AAC	P-GTTAGATCGGAAGAGCGGTTCAGCAGGAATGCCGAG	ACACTCTTTCCCTACACGACGCTCTTCCGATCTAACT
BC12-ATT	P-AATAGATCGGAAGAGCGGTTCAGCAGGAATGCCGAG	ACACTCTTTCCCTACACGACGCTCTTCCGATCTATTT
BC13-TAG	P-CTAAGATCGGAAGAGCGGTTCAGCAGGAATGCCGAG	ACACTCTTTCCCTACACGACGCTCTTCCGATCTTAGT
BC14-TTA	P-TAAAGATCGGAAGAGCGGTTCAGCAGGAATGCCGAG	ACACTCTTTCCCTACACGACGCTCTTCCGATCTTTAT
BC15-CCA	P-TGGAGATCGGAAGAGCGGTTCAGCAGGAATGCCGAG	ACACTCTTTCCCTACACGACGCTCTTCCGATCTCCAT
BC16-CGG	P-CCGAGATCGGAAGAGCGGTTCAGCAGGAATGCCGAG	ACACTCTTTCCCTACACGACGCTCTTCCGATCTCGGT
BC17-GCC	P-GGCAGATCGGAAGAGCGGTTCAGCAGGAATGCCGAG	ACACTCTTTCCCTACACGACGCTCTTCCGATCTGCCT
BC18-GGT	P-ACCAGATCGGAAGAGCGGTTCAGCAGGAATGCCGAG	ACACTCTTTCCCTACACGACGCTCTTCCGATCTGGTT
PE	CAAGCAGAAGACGGCATACGAGATCGGTCTCGGCATTCC	AATGATACGGCGACCACCGAGATCTACACTCTTTCCCT

hMeDIP Library Sequencing and Mapping. Pooled hMeDIP libraries were sequenced on an Illumina HiSeq 2500. FastQ files were demultiplexed using the Barcode Splitter on Galaxy (all mapping programs were run using Galaxy (Afgan et al., 2016). Demultiplexed samples were mapped to the mouse genome (mm9) using Bowtie2 (Langmead and Salzberg, 2012) with default settings. Duplicate reads were removed from the Bam files.

Differentially 5-hydroxymethylated Region (DhMR) Detection. Regional differences in hMeDIP enrichment between samples was determined using MACS2 (Feng et al., 2012). Aging-induced DhMRs used 3 month old mice and 18 month old mice. Overexpression (OE)-induced DhMRs used control lentivirus-injected brains and OE injected brains. A q-value of 0.05 was used as a cutoff for determining the significance of a peak. DhMRs located within chr*N*_random and chrUn_random (regions that cannot be confidently anchored to specific locations within the mouse genome build), and chrM were excluded from further analysis.

Genetic Element Enrichment. DhMRs identified by MACS2 for each sample, as well as those lost during aging or gained by Tet2 overexpression were mapped to a list of genetic elements (intragenic, intergenic, 5K promoter, exons, and introns). The enrichment of DhMRs in identified elements over the expected number was calculated. The expected DhMRs per element was calculated by finding the fraction of the genome covered by that element, multiplying that by the total number of DhMRs to derive the expected number of DhMRs for that element, then dividing the number of DhMRs mapped to each element by the expected number in that element to find the enrichment value. As a control, randomized DhMRs for each sample underwent these calculations, showing no enrichment over the expected values.

Gene Ontology Analysis. DhMRs were paired with overlapping RefSeq genes, and if the DhMRs was intergenic, it was paired with the nearest gene. Gene ontology analysis was performed using PANTHER (Mi et al., 2017) (www.geneontology.org) with RefSeq genes as the reference list (background). P-values were corrected using the Bonferroni method. Gene ontology terms that had greater than or equal to two-fold enrichment and a P-value of 0.05 or less after multiple hypothesis correction were considered significant; the top ten terms were shown in the figures.

hMeDIP-Seq Metagene Models. Metagene models were constructed using Deeptools (Ramirez et al., 2016). A 5bp binned BigWig file that was FPKM normalized (excluding ChrM, ChrY, Chr*N*_Random and ChrUn) was generated for each sample using bamCoverage. For generating a coverage scatterplot, the hMeDIP BigWig files were reads were quantified in 50kb bins using multiBigwigSummary. Metagene models were generated by scoring the BigWig files over RefSeq genes (that were scaled to the same size) or promoters using computeMatrix. Scores were averaged for every gene to arrive at the metagene model.

Data and statistical analyses. All experiments were randomized and blinded by an independent researcher before stereotaxic injection or assessment of genetic mouse models. Researchers remained blinded throughout histological,

biochemical and behavioral assessments. Groups were un-blinded at the end of each experiment upon statistical analysis. Data are expressed as mean ± s.e.m. The distribution of data in each set of experiments was tested for normality using D'Agostino-Pearson omnibus test or Shapiro-Wilk test. Statistical analysis was performed with Prism 7.0 software (GraphPad Software). Means between two groups were compared with two-tailed, unpaired Student's *t*-test. Comparisons of means from multiple groups with each other or against one control group were analyzed with one-way ANOVA followed by appropriate *post hoc* tests (indicated in figure legends).

SUPPLEMENTAL REFERENCES

Afgan, E., Baker, D., van den Beek, M., Blankenberg, D., Bouvier, D., Cech, M., Chilton, J., Clements, D., Coraor, N., Eberhard, C., et al. (2016). The Galaxy platform for accessible, reproducible and collaborative biomedical analyses: 2016 update. Nucleic Acids Res 44, W3-W10.

Alamed, J., Wilcock, D.M., Diamond, D.M., Gordon, M.N., and Morgan, D. (2006). Two-day radial-arm water maze learning and memory task; robust resolution of amyloid-related memory deficits in transgenic mice. Nat Protoc 1, 1671-1679.

Feng, J.X., Liu, T., Qin, B., Zhang, Y., and Liu, X.S. (2012). Identifying ChIP-seq enrichment using MACS. Nat Protoc 7, 1728-1740.

Langmead, B., and Salzberg, S.L. (2012). Fast gapped-read alignment with Bowtie 2. Nat Methods 9, 357-359.

Mi, H., Huang, X., Muruganujan, A., Tang, H., Mills, C., Kang, D., and Thomas, P.D. (2017). PANTHER version 11: expanded annotation data from Gene Ontology and Reactome pathways, and data analysis tool enhancements. Nucleic Acids Res 45, D183-D189.

Ramirez, F., Ryan, D.P., Gruning, B., Bhardwaj, V., Kilpert, F., Richter, A.S., Heyne, S., Dundar, F., and Manke, T. (2016). deepTools2: a next generation web server for deep-sequencing data analysis. Nucleic Acids Res 44, W160-165.

Smith, L.K., He, Y., Park, J.S., Bieri, G., Snethlage, C.E., Lin, K, Gontier, G., Wabl, R., Plambeck, K.E., et al. (2015). β2-Microglobulin is a systemic pro-aging factor that impairs cognitive function and neurogenesis. Nat Medicine 21, 932-937.